



Numerical simulation and method study of X-ray litho-density logging

Hua-Wei Yu^{1,2} · Yu-Xin Zhang² · Xiang-Hong Chen² · Wen-Ding Wang² · Chao-Zhuo Liu³

Received: 19 July 2020 / Revised: 12 October 2020 / Accepted: 13 October 2020 / Published online: 5 December 2020
© China Science Publishing & Media Ltd. (Science Press), Shanghai Institute of Applied Physics, the Chinese Academy of Sciences, Chinese Nuclear Society and Springer Nature Singapore Pte Ltd. 2020

Abstract To effectively replace the isotope radiation source in litho-density logging, this study presents a method for measuring the formation density and photoelectric absorption index (P_e) using a switchable X-ray tube. First, the gamma-ray litho-density logging (GLD) method for measuring formation density and P_e using chemical sources is introduced. Then, a benchmark verification based on the X-ray litho-density logging tool prototype and data published by Simon (In: Paper presented at the SPWLA 59th annual logging symposium, London, UK, 2018) was carried out using Monte Carlo numerical simulations. Second, the impacts of the photoelectric effect and detector statistical error on the GLD method were analyzed. Finally, based on a theoretical analysis, the formation density and P_e measurement algorithm (double energy window (DEW) method) was improved, which was found to be suitable for X-ray litho-density logging. Moreover, the results obtained using this algorithm were

compared with those obtained using the GLD method. The results indicate that owing to the impact of photoelectric effect and detector statistical error on the density energy window, the accuracy of formation density and P_e measurement using the GLD method is relatively low, with the uncertainty in formation density and P_e measurement reaching $2.620 \pm 0.047 \text{ g/cm}^3$ and $4.090 \pm 0.580 \text{ b/e}$, respectively. In comparison, the DEW method can improve the accuracy of density and P_e measurement to 0.006 g/cm^3 and 0.065 b/e , respectively, as the photoelectric effect in the density window is corrected using the counts in the lithology window of the energy spectrum. This study aims to provide a new theoretical foundation for processing X-ray litho-density logs in the future.

Keywords X-ray controllable source · Litho-density logging · Monte Carlo simulation

This work was partly supported by the National Natural Science Foundation of China (Nos. 41674129, 41874147), National Science and Technology Major Project of the Ministry of Science and Technology of China (No. 2017ZX05009-001), Fundamental Research Funds for Central Universities (No. 19CX02004A), and National Key Research and Development Program of China (No. 2016YFC0302800).

✉ Yu-Xin Zhang
943645309@qq.com

¹ Key Laboratory of Deep Oil and Gas, China University of Petroleum (East China), Qingdao 266580, China

² School of Geosciences, China University of Petroleum (East China), Qingdao 266580, China

³ College of Science, China University of Petroleum (East China), Qingdao 266580, China

1 Introduction

In traditional litho-density logging, ^{137}Cs , a gamma-ray radiation source, is used to measure formation density and photoelectric absorption index P_e . A commonly used method is to divide the gamma-ray spectrum into two energy windows, namely density window and lithology window, to measure formation density using the counts in the density window [1] and determine P_e using the ratio of counts in the lithology window to those in the density window. This method satisfies the precision requirements of litho-density logging and only requires a minimum of two or three test data points on the tool calibration. Currently, this is the main method used by oilfield service companies.

To eliminate the hazards associated with the use of an isotope radiation source, Becker et al. and King et al. first proposed a method to measure formation density using an electron linac as an X-ray source to replace chemical gamma-ray sources [2, 3]. However, an electron linac is too bulky to be used in borehole environments with diameters as small as 6 in. Therefore, a method of neutron-induced gamma density (NGD) logging using a D-T neutron generator was introduced twenty years ago [4–7]. In the last several years, X-ray density logging method has started attracting more interest with the advances in downhole X-ray generator technology. Badruzzaman compared the responses of NGD logging and X-ray density logging through theoretical studies and numerical simulations and concluded that an X-ray source is a more stable than a neutron-induced secondary gamma source, which is generated by an inelastic scattering of high-energy neutrons from a D-T generator [8]. Wraight et al. and Tkabladze et al. compared the measuring principles of X-ray density logging and Cs-137 source density logging (GLD method) and concluded that these two methods are similar in that both determine formation density using the gamma-ray counts within Compton windows and compute P_e using the ratio of the counts in two energy windows [9, 10]. Subsequently, Yu concluded that an X-ray energy spectrum is continuously distributed and its photon energy is generally much lower than that of Cs-137; moreover, the photoelectric effect contributes to the gamma-ray counts in the Compton window [11]. Therefore, formation density measurement from the Compton density window alone would be significantly affected by lithology.

Our work aims to improve the accuracy of formation density and P_e measurement using an X-ray source. We reviewed the published study by Simon et al. [12] on the response of an X-ray density logging instrument. We also performed Monte Carlo simulations, analyzed the energy spectra characteristics of X-rays, and evaluated the impact of the counts in the Compton density window on the formation density and P_e accuracies. Finally, we proposed a new formation density and P_e calculation method (double energy window (DEW) method) for X-ray litho-density logging and compared the processing results with the traditional GLD method.

2 Gamma-ray lithology density logging method

Lamarsh and Baratta suggested that in rock formations with a high P_e index, the lithology effect on bulk density computations can be minimized by increasing the energy threshold from 0.15 MeV to 0.24 MeV [13]. The electron density index calculation formula is as follows:

$$\rho_e = a \cdot \ln(N_H) + b, \quad (1)$$

where a and b are coefficients obtained from tool calibration and N_H denotes the counts in the density window. For limestone formation saturated with freshwater, the relationship between its bulk density ρ_b and electron density index ρ_e has been expressed by Ellis [14]:

$$\rho_b = 1.0704 \rho_e - 0.1883. \quad (2)$$

According to Bertozzi, Ellis, and Wahl [15], the photoelectric absorption index P_e is obtained from the ratio between the counts in the lithology window N_L and the counts in the density window N_H and is expressed by η ; its calculation formula is as follows:

$$P_e = \frac{A}{\eta + B} + C. \quad (3)$$

In formula (3), A , B , and C are tool-specific calibration coefficients.

3 X-ray density logging model and energy spectrum analysis

3.1 Calculation model and benchmark

An X-ray logging tool model (Fig. 1) was built using the MCNP5 code based on the ENDF70 nuclear data library. This tool is similar to the X-ray litho-density logging tool published by Simon et al. and Qu et al. [12, 16], and a high voltage of 350 kV is applied across the cathode and gold target of the anode in X-ray tubes. The theoretical tool responses were simulated in sandstone and limestone formations of varying porosities [17, 18]. A 20.16-cm-diameter borehole was filled with freshwater with a density of 1.0 g/cm^3 . The formation was cylindrical with a radius of 100 cm and a height of 180 cm. The tool has two gamma-ray detectors located at different distances from the source. The source-to-near detector spacing was 11 cm, and the far

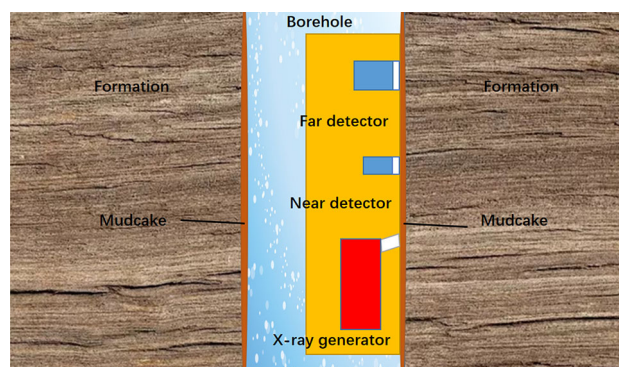


Fig. 1 (Color online) Tool-borehole-formation Monte Carlo calculation model

detector spacing was 22 cm. In some cases, there was a thin mudcake between the tool and the formation. To ensure the reliability of the calculated results, 4×10^9 photons were sampled and the statistical errors were reduced to a level below 1.0% using IMP cards during each simulation. The MCNP simulated the X-ray energy spectrum, as shown in Fig. 2. The response of the far detector, which was approximately equal to that of the D4 detector in the study by Simon et al. [12], is shown in Fig. 3.

As shown in Fig. 3, the simulation data of the far detector in this study and the D4 detector were benchmarked with the data simulated by Simon et al. [12]. The relationship between the density window (0.15–0.35 MeV) was simulated in various sandstone and limestone formations; the formation bulk density is basically the same as that obtained by Simon et al., which demonstrates that the results of the proposed numerical simulation in this study are reliable and can be used for subsequent studies on density and P_e measurement methods [12].

3.2 X-ray energy spectrum and cross-section analysis

To detailedly study the principle of formation density and P_e measurement using X-ray, the X-ray energy spectrum received by the detectors was first analyzed. Then, the detector responses in dolomite, limestone, and sandstone formations with an electron density of 2.341 g/cm^3 and respective P_e levels of 4.53 b/e, 2.72 b/e, and 1.64 b/e were obtained using the tool model (Fig. 1). The energy spectra of the scattering X-rays were also obtained, as shown in Fig. 4.

As shown in Fig. 4, when the photon energy is lower than 0.1 MeV, the count rate varies significantly in different formations and is sensitive to lithology. As photon energy increases, the difference in counts in the three

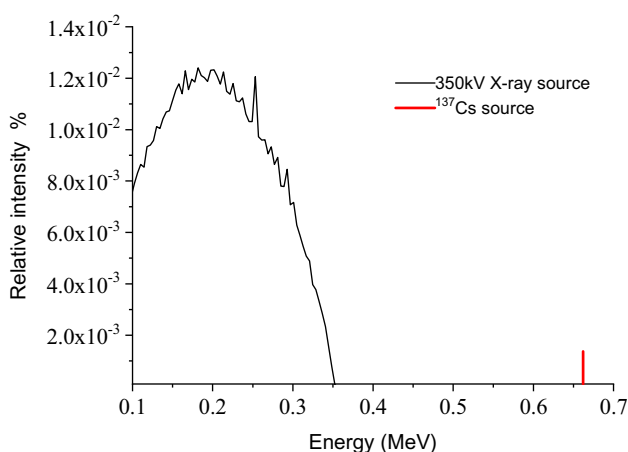


Fig. 2 X-ray energy spectrum released by 350 kV X-ray tube

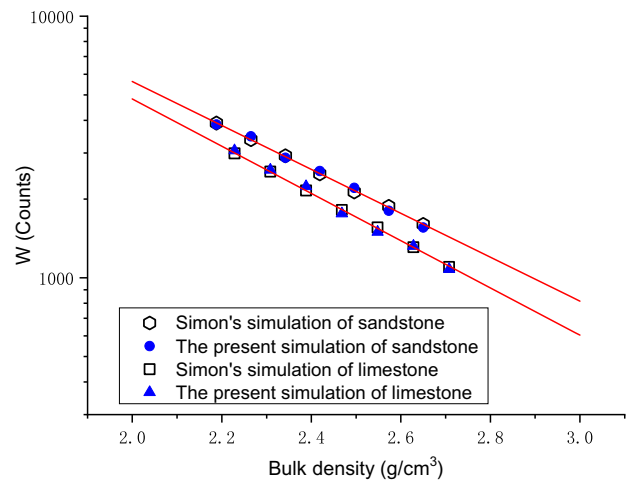


Fig. 3 (Color online) Logarithm of counts in the high-energy (0.15–0.35 MeV) window vs. density for simulation of this paper's far detector and simulation of Simon's D4 detector

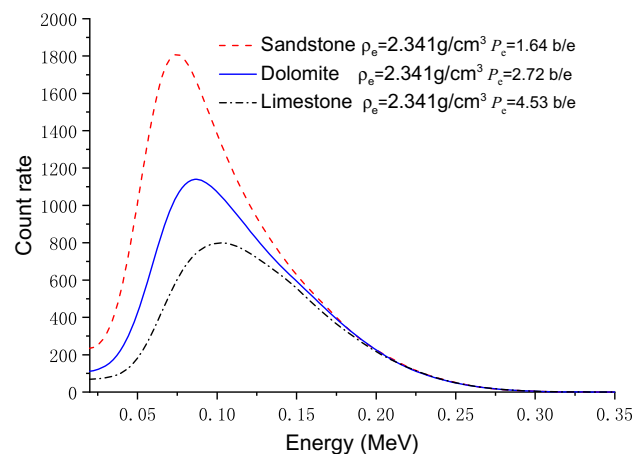


Fig. 4 (Color online) Scattering X-ray energy spectra of far detector in sandstone, limestone, and dolomite formations with the same density

formations decreases gradually and the curves of count rates overlap. For the two density windows that are commonly used in chemical source density logging, when the photon energy is within the range of 0.15–0.24 MeV, the count rates are high, but there is a certain difference in the count rates of the three formations. This is because the photons whose energies are within this range not only undergo Compton scattering (density), but are also affected by the photoelectric effect [19, 20], while photons with energies higher than 0.24 MeV basically undergo Compton scattering only and are not significantly affected by the photoelectric effect. Therefore, the counts in the three formations basically overlap. However, the count rates are quite low, indicating a large statistical error. If only photons with energies higher than 0.24 MeV are used to

calculate density, the calculation accuracy cannot meet the project requirements.

In order to determine the extent to which the counts in different energy windows are affected by the photoelectric effect of X-ray litho-density logging, the ratios R (%) of the photoelectric absorption coefficient μ_{ph} to the total attenuation coefficient μ (sum of Compton attenuation coefficient μ_c and photoelectric absorption coefficient μ_{ph}) with respect to the cross sections of the three formations were calculated using photons with energies within a range of 0–0.35 MeV. The calculation results are listed in Table 1.

From Table 1, it can be seen that when the limestone formation is selected as the reference formation, there is a difference of 1.58% in the values of R in the energy range of 0.15–0.35 MeV for the sandstone formation and 0.53% in the energy range of 0.24–0.35 MeV for the limestone formation; the former is nearly three times the latter, indicating that the impact of photoelectric effect (lithology) on the counts in the energy range of 0.15–0.35 MeV is three times its impact on the counts in the energy range of 0.24–0.35 MeV. However, the counts in the former range are much more (approximately 20 times) than the counts in the latter.

4 GLD method processing results

In order to detailedly study the applicability of GLD method for X-ray litho-density logging, the impact of photoelectric effect and detector statistical error on density window introduced by Ellis was analyzed using the MNCP simulation data which had been processed through a benchmark verification [14]. These two influential factors restrict the use of GLD method in X-ray litho-density logging.

4.1 Impact of photoelectric effect

The 350 kV X-ray generator released X-rays in the 0–0.35 MeV continuous energy spectrum into the formation; the X-rays interacted with the formation in the form of photoelectric effect and Compton scattering and were

received by the detectors. Formation density and P_e were calculated using formulas (1–3); the selected energy range in the lithology window was 0.04–0.08 MeV, and the threshold energy in the density window was generally 0.15 MeV. In order to verify the impact of photoelectric effect on GLD method during X-ray litho-density logging, the responses of the logging tool (Fig. 1) in sandstone, limestone, and dolomite formations with 0–30% porosity saturated with water were simulated. Then, based on the scattering X-ray energy spectra received by the detectors, the counts in the lithology window (0.04–0.08 MeV) and the counts in the density window (0.15–0.35 MeV) were respectively calculated, which were then, respectively, substituted into formulas (1, 3) to calculate formation density and P_e . The calculation results are shown in Fig. 5.

In practical cases of litho-density logging, limestone formation is usually selected as the reference formation. For sandstone, limestone, and dolomite formations, the density values calculated using formulas (1,2) differed significantly from the values obtained through simulation; particularly for the sandstone formation, the mean error was 0.075 g/cm³, and the maximum error was 0.093 g/cm³. The formation P_e calculated using formula (3) for the lithology window (0.04–0.08 MeV) and density window (0.15–0.35 MeV) differed significantly from the actual formation P_e , and the mean error of the measured P_e of the three formations was 0.21 b/e. For X-ray litho-density logging, the counts in the density window (0.15–0.35 MeV) are affected by the photoelectric effect. For this reason, the accuracy of density measurement by the GLD method in X-ray litho-density logging was low.

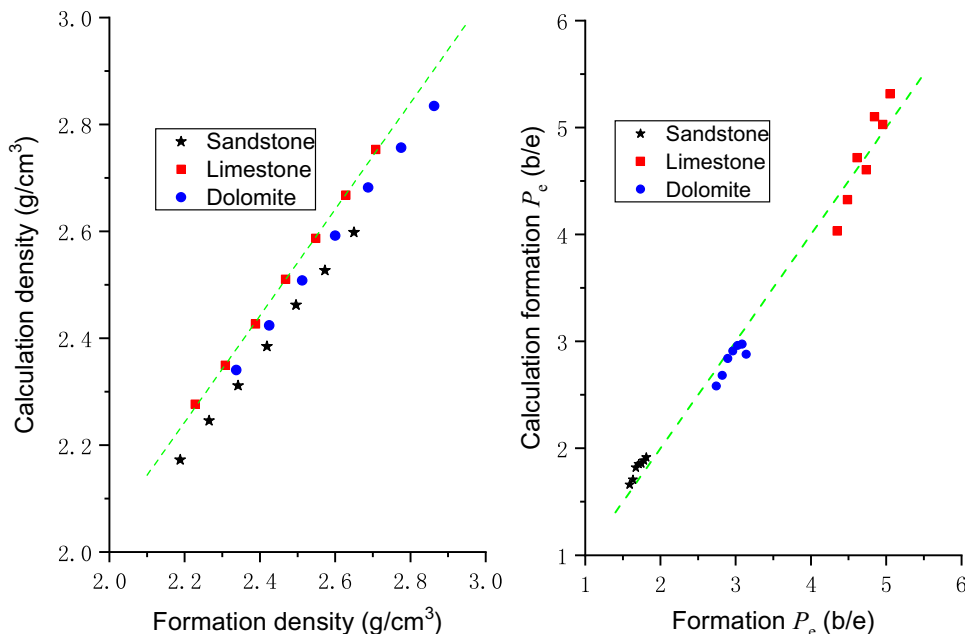
4.2 Impact of statistical error

Knoll observed a statistical error with respect to the receipt of photons by the detectors under the same measurement environment, that is, $\Delta N = \sqrt{N}$, where N denotes the counts received by the detectors [21]. Based on formulas (1,3), density measurement uncertainty $\Delta\rho$ and P_e measurement uncertainty ΔP_e can be expressed as

Table 1 R (%) values of three different formations

Formation	0.15 MeV R (%)	0.24 MeV R (%)	0.35 MeV R (%)	0.15–0.35 MeV		0.24–0.35 MeV	
				Mean R (%)	Counts	Mean R (%)	Counts
Sandstone	1.74	0.48	0.20	0.97	2,288	0.34	131
Dolomite	3.23	0.89	0.35	1.79	2,238	0.62	128
Limestone	4.60	1.26	0.49	2.55	2,129	0.87	126

Fig. 5 (Color online) Comparison between formation properties calculated using GLD method (density window: 0.15–035 MeV) and assumed formation properties



$$\Delta\rho = \left| \frac{\partial f(N_H)}{\partial N_H} \right| \Delta N_H, \tag{4}$$

and

$$\Delta P_e = \left| \frac{\partial f(N_L, N_H)}{\partial N_L} \right| \Delta N_L + \left| \frac{\partial f(N_L, N_H)}{\partial N_H} \right| \Delta N_H, \tag{5}$$

where ΔN_L and ΔN_H denote the statistical errors of the counts in the lithology window and the density window, respectively, and $f(N_H)$ and $f(N_L, N_H)$ denote the functional relationship between formation density and N_H , and the functional relationship between P_e and N_L, N_H , respectively.

From the aforementioned energy spectrum analysis, it can be seen that the density window of 0.24–0.35 MeV is less affected by the photoelectric effect (lithology) than the density window of 0.15–0.35 MeV, but the counts are too low. In order to verify the impact of the density window statistical error on the GLD method during X-ray litho-density logging, the simulation data in Fig. 5 and the scattering X-ray energy spectra received by the detectors were used to calculate the counts in the lithology window (0.04–0.08 MeV) and the counts in the density window (0.24–0.35 MeV). In addition, the density measurement uncertainty $\Delta\rho$ and P_e measurement uncertainty ΔP_e were calculated using formulas (1, 4) along with formulas (3, 5). The calculation results are shown in Fig. 6. Based on “JJG. (Military) 42–2014 Specification for Calibration of Density Logging Tool”, Li et al. believed that the standard density measurement uncertainty $\Delta\rho$ should be $\pm 1\%$ of the measured density value and the standard P_e measurement uncertainty should be ± 0.1 b/e [22].

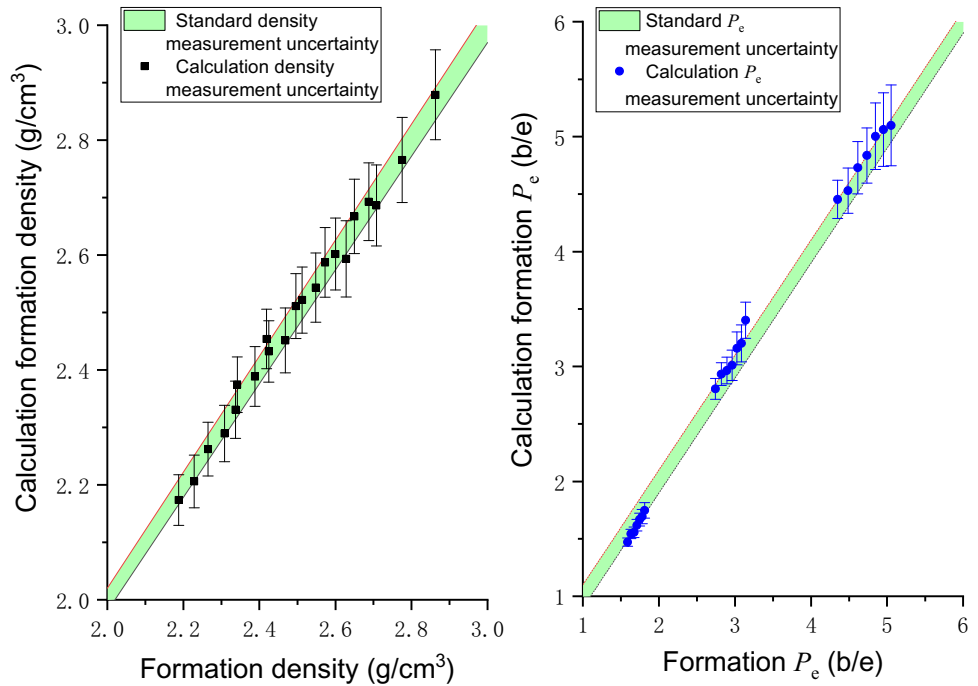
From Fig. 6, it can be seen that when the lithology window is 0.04–0.08 MeV and the density window is 0.24–0.35 MeV, the accuracy of density and P_e calculation using formulas (1–3) increases, but the measurement uncertainties do not meet the requirements. The analysis reveals that the impact of photoelectric effect on the GLD method can be reduced by choosing a density window of 0.24–0.35 MeV. However, owing to the low counts in this density window, the detector statistical error has a significant impact on the formation density and P_e calculation using the GLD method, and the density measurement uncertainty and P_e measurement uncertainty are not within the range of the specified measurement uncertainty levels.

The above analysis indicates that the number of scattering photons received by the detectors is directly proportional to the measuring time; the longer the measuring time, the smaller the detector statistical error will be. Table 1 shows that the count received by the detector in the 0.15–0.35 MeV energy window is 20 times the count in the 0.24–0.35 MeV energy window at a fixed measuring time. In order to reduce the uncertainty of density and P_e calculations based on the counts in the density window (0.24–0.35 MeV), the detector measuring time needs to be significantly increased, which means the logging speed will be reduced significantly.

5 Principle of DEW method

In X-ray litho-density logging, the impacts of photoelectric effect and detector statistical error on the density window result in low measurement accuracy of the GLD

Fig. 6 (Color online) Comparison between measurement uncertainties of GLD method (density window: 0.24–0.35 MeV) and specified measurement uncertainties



method. Therefore, this study proposes a method to calculate formation density and P_e , and improve the accuracy of X-ray litho-density logging. The counts in the density window subject to the impact of photoelectric effect are corrected using the counts in the lithology window to calculate the formation density accurately. When formation P_e is calculated, the counts in the lithology window subject to the impact of Compton scattering are corrected using the counts in the density window.

5.1 Density calculation

Simon et al. and Yu et al. believed that X-rays in X-ray litho-density logging can be characterized by lower energy and continuity when compared with 0.662 MeV gamma rays, and the impact of photoelectric effect on the counts in the density window should not be neglected [11, 12]. Then, the relationship between the counts in the density window N_H and the counts in the lithology window N_L can be expressed as

$$N_H = N_0 e^{-(\mu_{ph,E_H} + \mu_{c,E_H})d}, \tag{6}$$

$$N_L = N_0 e^{-(\mu_{ph,E_L} + \mu_{c,E_L})d}, \tag{7}$$

where photoelectric absorption coefficients $\mu_{ph,E_H} = Ka(E_H)\frac{N_A}{2}U$, $\mu_{ph,E_L} = Ka(E_L)\frac{N_A}{2}U$; Compton attenuation coefficients $\mu_{c,E_H} = b(E_H)\frac{N_A}{2}\rho_e\sigma_{c,e}$, $\mu_{c,E_L} = b(E_L)\frac{N_A}{2}\rho_e\sigma_{c,e}$; and d is the distance of the source from the detector. K is a constant whose value depends on the photon energy and unit of the cross section; $a(E)$ and

$b(E)$ are related to X-ray energy, respectively; E_H and E_L represent the high and low energy in the X-ray energy spectrum, respectively; $\sigma_{c,e}$ denotes the electron scattering cross section (electron scattering cross sections of commonly seen formation materials are basically equal); N_A denotes the Avogadro constant; and U is a volumetric photoelectric absorption index defined as $\rho_e \cdot P_e$. According to Yu et al. [11], the electron density response formula can be obtained as follows:

$$\rho_e = a + b \ln(N_H) + c \ln(N_L). \tag{8}$$

When the lithology and density windows are fixed, a , b , and c are constants and can be obtained from a tool experiment or through a simulation. The calculated electron density is substituted into formula (2) to calculate the measured density (apparent density).

Equation (8) in this study for X-ray litho-density logging is similar to the density correction equation, which was introduced by Ellis et al. [1] for the Cs-137 source litho-density logging; however, it is not widely used for this purpose. Both Ellis et al. and Serra et al. [14, 23] believed that when formulas (1, 2) are used to calculate the formation density in Cs-137 source density logging, the lithological effect could be eliminated by controlling the boundary of the density window. Its statistical precision and potential well logging speed can meet the engineering requirements.

The previous analysis indicates that as the energy of X-rays released by the X-ray generator is always lower than the energy of gamma rays released by Cs-137, its statistical accuracy will be significantly reduced by

increasing the boundary of the density window, and its potential measuring speed will also be reduced. Therefore, formulas (1, 8) can be used to calculate the formation density in X-ray litho-density logging.

In general, mudcake has a significant effect on density logging, and it is generally corrected by a spine and ribs chart. Similarly, formulas (1, 8) are used to calculate the near- and far-spacing densities, and a spine and ribs chart is developed to correct the effect of mudcake in X-ray litho-density logging, as shown in Fig. 7. The “spine” is the locus of near- and far-spacing densities without mudcake, and the “ribs” trace the two densities for the presence of an intervening mudcake. The physical parameters of different types of mudcake are shown in Table 2.

In Fig. 7, the red rib points are acquired in the 30% water-saturated sandstone formation, and the blue rib points are acquired in the 5% water-saturated limestone formation. The mudcake density range is 1–2.44 g/cm³, P_e range is 0.36–109.60 b/e, and mudcake thickness is up to 1.6 cm. Therefore, the effect of mudcake on density measurement can be corrected by using the spine and ribs chart in X-ray litho-density logging.

5.2 P_e calculation

The photoelectric absorption coefficient μ_{ph} is based on the cross sections of quartz, calcite, and dolomite materials commonly seen in well logging, and the relationship is shown in Fig. 8.

The photoelectric absorption coefficient and photo energy (0.02 ~ 0.5 MeV) in the same formation are directly proportional to each other in a log–log coordinate system [14]; then, we have the following relationship:

$$\frac{\ln \mu_{ph,L}}{\ln \mu_{ph,H}} = \frac{\ln(E_L)}{\ln(E_H)} = \alpha. \tag{9}$$

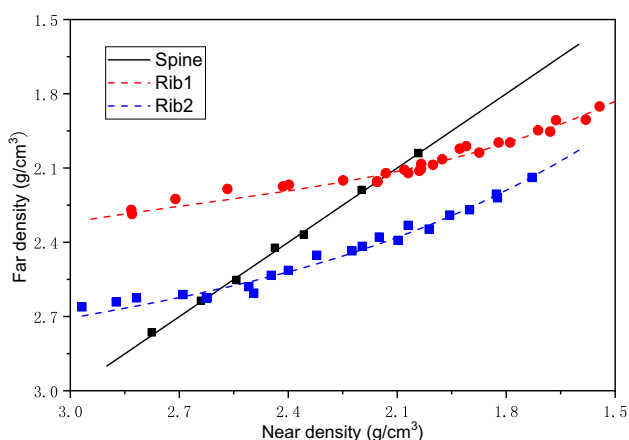


Fig. 7 (Color online) Spine and ribs chart of the X-ray litho-density tool for mudcakes

So that $\mu_{ph,L}$ can be expressed as:

$$\mu_{ph,L} = \mu_{ph,H}^\alpha. \tag{10}$$

When density and lithology windows are fixed, α is a constant, and formulas (6, 7 and 10) can be simplified as follows:

$$A_p U^\alpha + B_p U = C_p \ln(N_L) + D_p \ln(N_H) + F_p, \tag{11}$$

where C_p and D_p relate to the attenuation distance d of energy E ; F_p relates to energy E and initial photon flux; and A_p and B_p only relate to energy. From formulas (6, 7), $A_p U^\alpha$ and $B_p U$ are primarily related to $\mu_{ph,L}$ and $\mu_{ph,H}$, respectively. As shown in Fig. 8, $\mu_{ph,L}$ is two orders of magnitude larger than $\mu_{ph,H}$. Therefore, $A_p U^\alpha$ is much greater than $B_p U$ and $B_p U$ can be deemed to be zero. Then, formula (11) can be transformed to:

$$U = (A \ln(N_H) + B \ln(N_L) + C)^D. \tag{12}$$

According to the relationship between volumetric absorption index U and P_e , we have:

$$P_e = U/\rho_e, \tag{13}$$

where $A, B, C,$ and D are constants which can be obtained from tool calibration or through simulation.

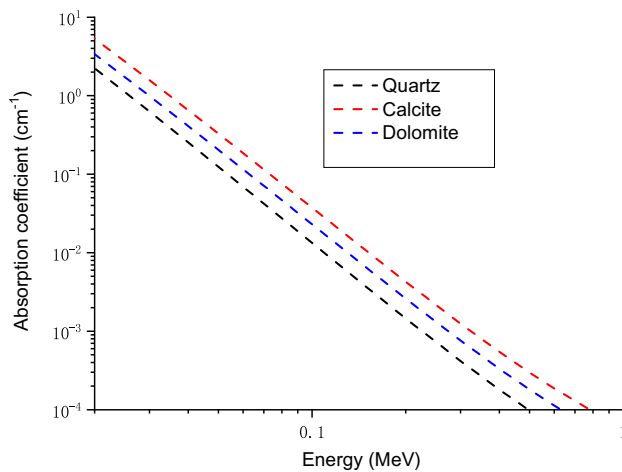
6 Results comparison between DEW and GLD method

In order to verify the ability of the DEW method proposed in this study for X-ray litho-density logging to significantly improve the measurement accuracy, the responses were simulated using the logging tool model not only in conventional formations (sandstone, limestone, dolomite) but also in complex lithological formations. The simulation data were used to calculate the counts in lithology window (0.04–0.08 MeV) and the counts in density window (0.15–0.35 MeV), which were then substituted into formulas (2, 8, 11, 12) to calculate formation density and P_e . The results of this method were compared with the results of GLD method (lithology window: 0.04–0.08 MeV, density window: 0.24–0.35 MeV). The petrophysical properties of the complex formations are listed in Table 3. Formations 1–5 are shale minerals, 6 and 7 are volcanic minerals, and 8 and 9 are salt rock minerals. A comparison of the results obtained using the two methods is shown in Fig. 7.

Figure 9 shows that for the aforementioned conventional formations, the maximum and mean density errors calculated using the GLD method are 0.035 g/cm³ and 0.023 g/cm³, respectively, and the P_e error is basically ± 0.2 b/e. However, for complex lithological

Table 2 Physical parameters of mudcakes

Composition	Density (g/cm ³)	P_e (b/e)
100% water (H ₂ O)	1.00	0.36
13% calcite (CaCO ₃) 87% water (H ₂ O)	1.22	0.97
39% calcite (CaCO ₃) 61% water (H ₂ O)	1.67	2.20
26.5% barite (BaSO ₄) 73.5% water (H ₂ O)	1.93	70.97
41% barite (BaSO ₄) 59% water (H ₂ O)	2.44	109.60

**Fig. 8** (Color online) Relationship between Photoelectric absorption coefficient μ_{ph} and photo energy**Table 3** Formation rock petrophysical properties

No	Formation	Density (g/cm ³)	P_e (b/e)
1	Kaolinite	2.62	1.63
2	Biotite	2.95	6.22
3	Smectite	2.13	3.22
4	Clinochlore	2.67	1.38
5	Illite	2.75	4.37
6	Diorite	2.86	4.58
7	Gabbro	2.90	5.99
8	Carnallite	1.64	4.09
9	Anhydrite	2.95	5.05

formations, the errors of formation density and P_e calculated using the GLD method are higher; the maximum density error is 0.047 g/cm³ and the maximum P_e error is 0.58 b/e. However, the DEW method significantly improves the accuracy of formation density and P_e calculation than the GLD method. For both conventional and complex lithological formations, the mean density measurement error of the DEW method is 0.006 g/cm³, which is nearly three times lower than that of the GLD method, the error of P_e is within 0.1 b/e, and the mean error of P_e is

0.065 b/e, which is nearly two times lower than that of the GLD method.

The above analysis indicates the detector statistical error will also affect the accuracy of density and P_e calculation. In this study, the impact of detector statistical error on calculation accuracy of the DEW method was analyzed, and the density measurement uncertainty and P_e measurement uncertainty of the DEW method were calculated. The results are shown in Fig. 10.

From Fig. 10, it can be seen that for conventional and complex lithological formations, the density measurement uncertainty of the DEW method proposed in this study arising from detector statistical error is smaller than 1%, and the P_e measurement uncertainty of the DEW method is also smaller than 0.1 b/e. Therefore, the impacts of detector statistical error on formation density and P_e measurement using the DEW method are within the specified ranges for litho-density logging. According to the above analysis, the DEW method can significantly improve the accuracy of formation density and P_e calculations without affecting the logging speed. This method provides a theoretical foundation for processing X-ray litho-density logging data in the future.

7 Discussion

In this study, the accuracy of the logging tool model and simulation data was verified by benchmarking them against Simon et al.'s [12] experimental data, and the scattering X-ray energy spectra in formations (conventional formations) with the same density and different lithological properties were analyzed. The counts in the density window of 0.24–0.35 MeV were subject to a smaller impact by the photoelectric effect and were relatively low, but were subject to a greater impact by the detector statistical error. The counts in the density window of 0.15–0.35 MeV were subject to smaller impact by the detector statistical error but were seriously affected by the photoelectric effect. Based on the results of X-ray litho-density logging data processing with the GLD method, the measuring accuracy of the GLD method was found to be low during the X-ray litho-density logging.

Fig. 9 (Color online)
Comparison between formation density and P_e calculated using the DEW method and those calculated using the GLD method

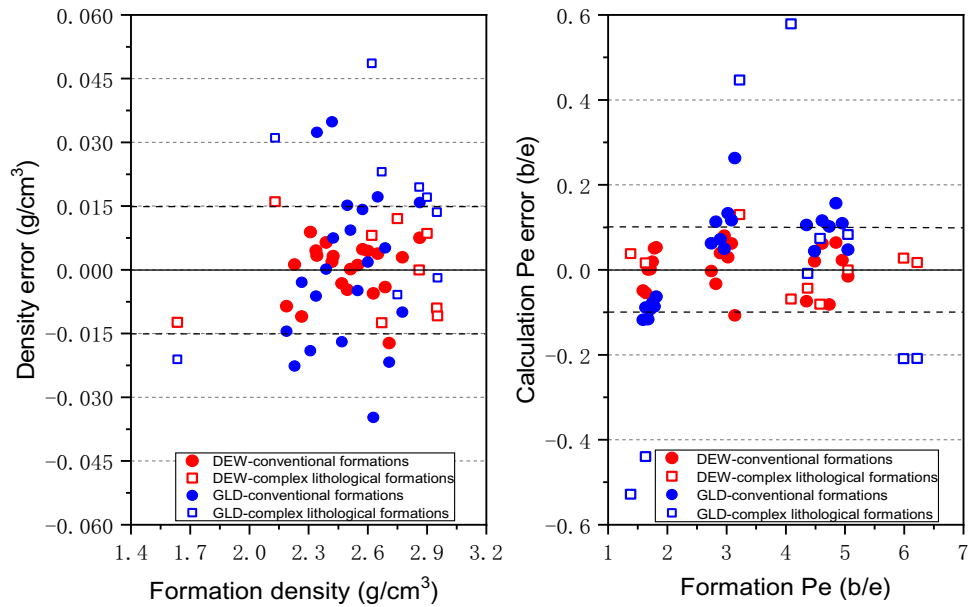
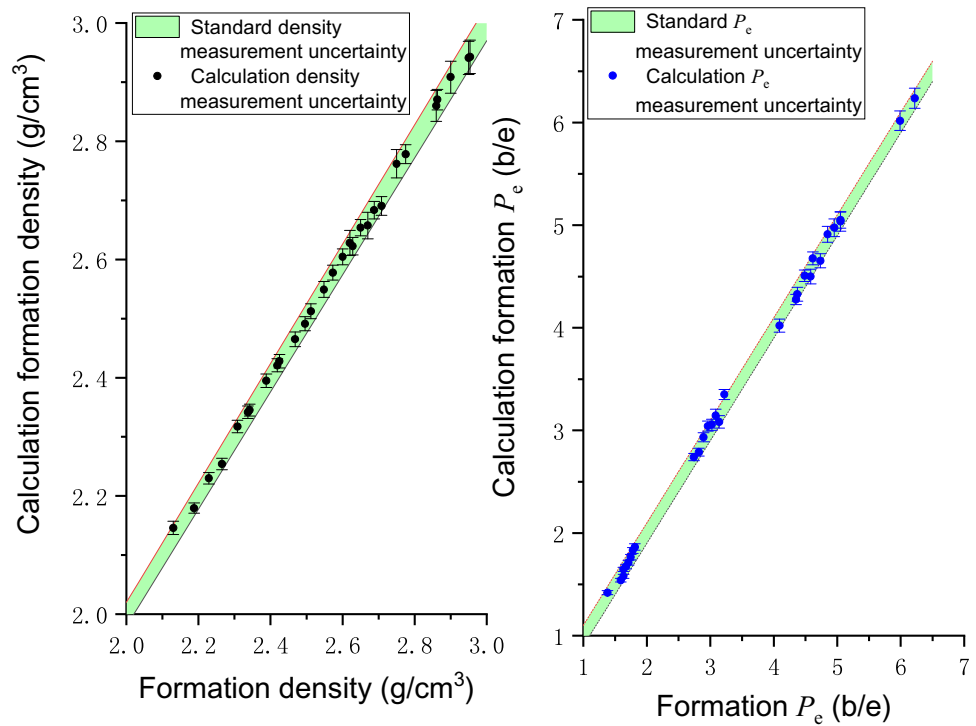


Fig. 10 (Color online)
Comparison between the measurement uncertainties of the DEW method and the specified measurement uncertainties



The DEW method was improved to calculate formation density and P_e during X-ray litho-density logging based on the relationship between the counts received by the detectors and formation density and P_e , analysis of the main contributions of the photoelectric effect and Compton scattering, and theoretical derivation. A traditional spine and ribs chart can also be used to effectively correct the influence of mudcake on X-ray litho-density logging. Compared with the GLD method, the DEW method

significantly reduced calculation errors and measurement uncertainties.

8 Conclusion

- (1) For litho-density logging using a 350 kV X-ray tube, a density window 0.15–0.35 MeV is better than

0.24–0.35 MeV for reducing the counting statistical error.

- (2) The DEW method proposed in this study for X-ray litho-density logging significantly improved the accuracy of formation density and P_e calculation. The simulation results show that the density calculation error is 0.006 g/cm^3 and the P_e calculation error is 0.065 b/e. The results indicate that the DEW method can accurately measure the density and P_e of both conventional and complex lithological formations during X-ray litho-density logging.
- (3) A spine and ribs chart, which is widely used in gamma-ray density logging, is also effective in compensating for the influence of mudcake on X-ray litho-density logging.

References

1. D. Ellis, C. Flaum, E. Marienbach et al., Litho-density tool calibration. *Soc. Petrol. Eng. J.* **25**(04), 515–520 (1985). <https://doi.org/10.2118/12048-PA>
2. A.J. Becker, J.R. Boyce, G.W. Corris et al., Detection of scattered X-rays from an electron linac in a borehole. *Nucl. Instrum. Meth. B* **24–25**, 995–998 (1987). [https://doi.org/10.1016/S0168-583X\(87\)80296-3](https://doi.org/10.1016/S0168-583X(87)80296-3)
3. G. King, A.J. Becker, G.W. Corris et al., Density logging using an electron linear accelerator as the x-ray source. *Nucl. Instrum. Meth. B* **24–25**, 990–994 (1987). [https://doi.org/10.1016/S0168-583X\(87\)80295-1](https://doi.org/10.1016/S0168-583X(87)80295-1)
4. R.D. Wilson, Bulk density logging with high-energy gammas produced by fast neutron reactions with formation oxygen atoms. In: *Proceedings of Nuclear Science Symposium and Medical Imaging Conference*, (San Francisco), 209–213 (1995) doi: <https://doi.org/https://doi.org/10.1109/NSSMIC.1995.504211>
5. R.C. Odom, S.M. Bailey, R.D. Wilson, et al., Pulsed neutron density measurements: modeling the depth of investigation and cased-hole wellbore uncertainties. In: *Proceedings of SPWLA 40th Annual Logging Symposium*, (paper JJ) (1999)
6. H.W. Yu, J.M. Sun, J. Wang et al., Accuracy and borehole influences in pulsed neutron gamma density logging while drilling. *Appl. Radiat. Isot.* **69**(9), 1313–1317 (2011). <https://doi.org/10.1016/j.apradiso.2011.04.023>
7. H.W. Yu, *The Fundamental Research of the Pulsed-Neutron Density Logging While Drilling* (China University of Petroleum (East China), Qingdao, 2011), pp. 30–36
8. A. Badruzzaman, An assessment of fundamentals of nuclear-based alternatives to conventional chemical source bulk density measurement. *Petrophysics* **55**(05), 415–434 (2014)
9. P. Wraight, A.J. Becker, J.L. Groves, et al., High voltage x-ray generator and related oil well formation analysis apparatus and method. U.S. Patent 7,991,111, 2 August 2011.
10. A. Tkabladze, X-Ray Generator Regulation with High Energy Tail Windows. U.S. Patent 10,007,024, 26 June 2018.
11. H.W. Yu, X.H. Chen, Y. Zhou et al., Impact of photoelectric effect on X-ray density logging and its correction. *Appl. Radiat. Isot.* **156**, 108785 (2020). <https://doi.org/10.1016/j.apradiso.2019.06.031>
12. M. Simon, A. Tkabladze, S. Beekman, et al., A Revolutionary X-Ray tool for true sourceless density logging with superior performance. Paper presented at the SPWLA 59th annual logging symposium, London, UK, 2018
13. J.R. Lamarsh, A.J. Baratta (eds.), *Introduction to Nuclear Engineering*, 3rd edn. (Prentice Hall, New Jersey, 2001).
14. D.V. Ellis, J.M. Singer (eds.), *Well Logging for Earth Scientists* (Elsevier, Holand, 1987).
15. W. Bertozzi, D.V. Ellis, J.S. Wahl, The physical foundation of formation lithology logging with gamma rays. *Geophysics* **46**(10), 1439–1455 (1981). <https://doi.org/10.1190/1.1441151>
16. S.S. Qu, Z. Guo, R.Z. Tai et al., Design of soft X-ray photon correlation spectroscopy device. *Nucl. Tech.* **42**(4), 040103 (2019). [https://doi.org/10.11889/j.0253-3219.2019.hjs.42.040103.\(inChinese\)](https://doi.org/10.11889/j.0253-3219.2019.hjs.42.040103.(inChinese))
17. M.J. Berger, J.H. Hubbell, *XCOM: Photon Cross Sections on a Personal Computer* (National Bureau of Standards, Gaithersburg, 1987). <https://doi.org/10.2172/6016002>
18. M.C. White, Photoatomic Data Library MCPLIB04: a new photoatomic library based on data from ENDF/B-VI Release 8, Los Alamos National Laboratory internal memorandum X-5:MCW-02–111(2002) https://mcnp.lanl.gov/BUGS/la-ur-03-1019_mcplib04.pdf
19. Y. Zhou, H.W. Yu, X.H. Chen et al., Study on near detector-source spacing of density logging based on the X-ray source. *Nucl. Tech.* **41**(12), 120401 (2018). <https://doi.org/10.11889/j.0253-3219.2018.hjs.41.120401> (in Chinese)
20. H.W. Yu, L. Zhang, B. Hou, Study on the impact of pair production interaction on D-T controllable neutron density logging. *Appl. Radiat. Isot.* **111**, 104–109 (2016). <https://doi.org/10.1016/j.apradiso.2016.01.030>
21. G.F. Knoll, *Radiation Detection and Measurement* (John Wiley, New Jersey, 1989).
22. F.L. Li, S.B. Guan, X.C. Tang et al., Evaluation of the uncertainties of the measurements of density logging tools. *Sci. Technol. Innov. Herald* **13**(10), 231–232 (2015)
23. L. Serra, O. Serra, *Well Logging: Data Acquisition and Applications* (Technips, Paris, 2004).